EUROPEAN ORGANIZATION FOR NUCLEAR RESEARCH

CERN-EP/85-199
9 December 1985

EVIDENCE FOR DIRECT pp INTERACTIONS IN THE FRAGMENTATION CHANNEL $p + \alpha \rightarrow p + pX$ AT $\sqrt{s} = 88$ GeV

W. Bell[1], K. Braune[2a], G. Claesson[3b], D. Drijard[1], M.A. Faessler[1], H.G. Fischer[1], H. Frehse[1c], R.W. Frey[4d], S. Garpman[3], W. Geist[1b], C. Gruhn[5], P. Hanke[6], M. Heiden[1b], W. Herr[6], P.G. Innocenti[1], T.J. Ketel[2e], E.E. Kluge[6], I. Lund[3], G. Mornacchi[1], T. Nakada[6d], I. Otterlund[3], M. Panter[1], B. Povh[2], A. Putzer[6], E. Stenlund[3], T.J.M. Symons[5], R. Szwed[2f] and O. Ullaland[1]

ABSTRACT

We have investigated kinematical correlations between the outgoing beam proton and the proton emerging from the fragmenting α-particle in $p\alpha$ collisions at $\sqrt{s_{p\alpha}} = 88$ GeV. Strong correlations are seen, indicating the dominance of quasi-elastic pp scattering in the fragmentation channel $p + \alpha \rightarrow p + pX$, for the $|t|$ range 0.05–1.00 $(GeV/c)^2$. A Monte Carlo simulation of this process can explain the observed correlation spectra assuming an admixture of about 16% spectator protons.

(Submitted to Zeitschrift für Physik C)

---

1) CERN, Geneva, Switzerland.
2) Max-Planck Institut für Kernphysik, Heidelberg, Fed. Rep. Germany.
3) Division of Cosmic and Subatomic Physics, University of Lund, Sweden.
4) Physikalisches Institut der Universität, Heidelberg, Fed. Rep. Germany.
5) Nuclear Science Division, Lawrence Berkeley Laboratory, Berkeley, Calif., USA.
6) Institut für Hochenergiephysik der Universität Heidelberg, Fed. Rep. Germany.
a) Now at SLAC, Stanford, Calif., USA.
b) Now at LBL, Berkeley, Calif., USA.
c) Now at Control Data Corporation, Zürich, Switzerland.
d) Now at SIN, Villigen, Switzerland.
e) Now at Natuurkundig Lab., Vrije Universiteit, Amsterdam, The Netherlands.
f) Now at Inst. of Exp. Physics, University of Warsaw, Poland.

1. INTRODUCTION

At relativistic energies, the de Broglie wavelength of a nucleon is much shorter than a typical internucleon distance. This implies that in a collision of two nuclei individual nucleons may be resolved. Fragmentation (or break-up) of a nucleus is a soft process involving four-momentum transfer $|t|$ of at most 1 $(GeV/c)^2$. At present it is not possible to describe such a soft process with Quantum Chromodynamics (QCD), and several models have been proposed to explain the process. Goldhaber [1] has assumed that the momentum distributions of the fragments are governed by the intrinsic momenta of nucleons prior to break-up. In contrast, Schmidt et al. [2] and Koonin and Collaborators [3] have given a relativistic hard-scattering model where the momentum distributions of the detected particles arise from direct constituent interactions (where the constituents are the nucleons).

Recently, Anderson et al. [4] have measured momentum distributions of break-up fragments at relativistic incoming energies (1–2 GeV per nucleon) for various beam and target combinations. They observe that the transverse momentum (p_T) distributions are wider than the longitudinal (p_L) ones when evaluated in the rest frame of the fragmenting nucleus. Such a behaviour persists at ultra-relativistic energies, as shown in a previous publication on $\alpha\alpha$ interactions [5].

The two mechanisms hitherto discussed can be examined in $p\alpha$ reactions, by looking at the correlation (or lack of it) between the momenta of the outgoing beam proton and that of a proton fragment emerging from the α particle. The data were obtained using the Split-Field Magnet (SFM) detector at the CERN Intersecting Storage Rings (ISR). The beam energies were 31 GeV for the proton beam and 15 GeV per nucleon for the α beam. The $p\alpha$ total centre-of-mass (c.m.) energy was $\sqrt{s_{p\alpha}} = 88$ GeV.

2. EXPERIMENT AND ANALYSIS

2.1 Set-up and trigger

The SFM detector consists of planar multiwire proportional chambers (MWPCs) arranged in such a way as to cover optimally the full solid angle. However, because of the beam pipes, high-momentum particles with polar angle deflections < 7 mrad from the beam directions could not be detected. The data presented here were taken with a fragmentation trigger. This trigger required one or two high-momentum charged-track candidates on both sides of the intersection and rejected events with low-momentum charged-track candidates (veto on central chambers at large angles to the beam directions).

2.2 Data analysis

The events were processed by the SFM reconstruction programs. The present analysis is based on 23000 inelastic $p\alpha$ events taken with the fragmentation trigger and where at least one track on each side had been reconstructed. To identify the fragments with charge number $Z = 1$ and $Z = 2$, dE/dx information from scintillator counters was used as in a previous analysis [5]. Furthermore, to distinguish proton fragments from deuterons and tritons ($Z = 1$), the following cuts in momentum (p^*) in the αp c.m. system (see Appendix A) were applied:

$$\begin{aligned} &\text{proton:} && 6 < p^* < 15 \text{ (GeV/c)}, \\ &\text{deuteron:} && 17 < p^* < 26 \text{ (GeV/c)}, \\ &\text{triton:} && 30 < p^* < 37 \text{ (GeV/c)}, \end{aligned}$$

and a beam proton was identified by $30 < p^* < 55$ (GeV/c).

In order to improve on the resolution, $\Delta p/p$ cuts (Δp is the uncertainty in the momentum from fitting the track) were applied, similar to those in the previous analysis [5]:

$$\begin{aligned} &\text{proton fragment:} \quad \Delta p/p \leq 0.06\,, \\ &\text{proton beam:} \quad \Delta p/p \leq 0.12\,. \end{aligned}$$

To study 'pure' nuclear break-up we further demanded that no negative tracks (mainly π^-) and no tracks with $p^* < 6$ (GeV/c) (mainly π^+ and to a minor extent non-diffractive protons) should exist in the event. This off-line requirement reduces the sample by only a few percent owing to the fact that already the multiplicity requirement in the hardware trigger strongly suppresses fragmentation channels with accompanying pions. Because of the trigger conditions and the acceptance of the detector, the four-momentum transfer (t) to the beam proton is limited to values $|t| > 0.05$ (GeV/c)^2.

2.3 Correlation functions

All the correlation functions are evaluated in the αp c.m. system. Let Φ^*_{pb} and Φ^*_{pf} denote the azimuthal angles of outgoing protons from the beam (b) and the fragmenting (f) α-particle, respectively. Furthermore, let $\xi^*_\Phi = \Phi^*_{pb} - \Phi^*_{pf}$ be the difference in azimuthal angle (if $\xi^*_\Phi < 0$, 2π is added). The distribution in ξ^*_Φ in the absence of correlations should be uniform for an ideal detector. Observe that with this definition the range of ξ^*_Φ is from 0 to 2π, i.e. one can distinguish whether the beam proton comes 'above' or 'below' the fragmentation proton in the azimuthal plane. This might be useful since the acceptance could vary for detecting two particles in the two cases. It is expected, however, that the distributions in ξ^*_Φ should be symmetric around π. In azimuthal angles we have studied $d^2N/d\Phi^*_{pf}d\Phi^*_{pb}$, the two-dimensional correlation function as well as the ratio of the one-dimensional distributions $(dN/d\xi^*_\Phi)_{eve}/(dN/d\xi^*_\Phi)_{mix}$. Here the subscripts eve and mix mean that the two tracks were taken from the same event and from different events, respectively. In the mixed event the beam proton from the first event was taken together with the fragmentation proton from the second, and so on. The event mixing is done in order to achieve an uncorrelated background. The dividing by $(dN/d\xi^*_\Phi)_{mix}$ cancels effects of acceptance in first order. Likewise, in the transverse momentum components p^*_x and p^*_z, we have defined the quantities $\xi^*_x = p^*_{x,pb} + p^*_{x,pf}$ and $\xi^*_z = p^*_{z,pb} + p^*_{z,pf}$, and studied the one-dimensional correlation functions $(dN/d\xi^*_x)_{eve}/(dN/d\xi^+_x)_{mix}$ and $(dN/d\xi^*_z)_{eve}/(dN/d\xi^*_z)_{mix}$.

The data sample used for the correlation study (and event mix) consisted of events where the outgoing beam proton and at least one fragmentation proton were identified. This sample was about 9000 events. The charge-exchange reactions and fragmentation channels like $\alpha \rightarrow d + d$ and $\alpha \rightarrow {}^3He + n$ are discarded, owing to the trigger requirement and momentum cuts. Furthermore, the $\Delta p/p$ demand of the detected particles reduces the original sample by 39%. Our final data sample thus contains the reaction channels:

$$p_b + \alpha \rightarrow p_b + p + X \qquad \text{and} \qquad p_b + \alpha \rightarrow p_b + p + p + X'$$

where X could be ${}^3H + k\pi^0$ and $d + n + k\pi^0$ whereas X′ could be $n + n + k\pi^0$ ($k = 0, 1, \ldots$).

3. EXPERIMENTAL RESULTS

3.1 Inclusive and semi-inclusive cross-section for the proton fragmentation channel

Since, as discussed earlier, the fragmentation trigger introduces a bias (only events with absolute four-momentum transfer $|t| > 0.05$ (GeV/c)^2 to the beam proton can be detected), a data set taken with a different trigger (minimum bias) was used to calculate the absolute cross-sections. This trigger required a minimum of one track candidate somewhere in the detector. A normalization was done to the αp production cross-section [6]. The measured proton inclusive fragmentation cross-section $\sigma(p + \alpha \rightarrow p + pX)$ is 71 $\pm$ 11 mb. If non-diffractive protons are subtracted using the proportionality to $(1 - x_F)$ a value of 55 $\pm$ 11 mb is obtained. If we reject events with one or more negative track(s) in the α rapidity hemisphere (c.m. system) and tracks with $p^* < 6$ GeV/c then the proton semi-inclusive fragmentation cross-section is 8 $\pm$ 2 mb.

3.2 Correlation spectra

In Fig. 1 the double-differential yield $d^2N/d\Phi^*_{pf}d\Phi^*_{pb}$ in azimuthal angles in the αp c.m. system is shown. There is a large concentration of almost 'back-to-back' correlated pairs ($\xi^*_\Phi = \Phi^*_{pb} - \Phi^*_{pf} \approx \pi$). The diagonal lines indicate the expectation for quasi-elastic scattering (QES) if the Fermi motion of the nucleons inside the α-particle, as well as the spreading due to resolution of the detector and to undetected π^0's, are ignored. It is obvious from the spectra that QES dominates but cannot alone reproduce all the observed features. The yields outside the QES region at $\xi^*_\Phi < \pi/2$ and $\xi^*_\Phi > 3\pi/2$ are about 8% of the total sample. This indicates a 'spectator proton' contribution of about 16% in the total sample. Using mixed events and normalized double-differential yields (see Section 2.3), it can be ruled out that acceptance causes the observed correlation. Furthermore, in Figs. 2a and 2b the spectra of proton fragments (not acceptance-corrected) are given as a function of transverse momentum squared (p_T^2) for two regions in ξ^*_Φ. The region $\pi/2 < \xi^*_\Phi < 3\pi/2$ is where QES takes place, whereas $\xi^*_\Phi < \pi/2$ and $\xi^*_\Phi > 3\pi/2$ is expected to be the region dominated by 'spectators' (SPE). Observe the strikingly different shapes of the experimental spectra; for QES, the spectrum is expected to decline close to $p_T^2 = 0.05$ (GeV/c)^2 because of the trigger condition on the beam proton side [the lower momentum cut of $|t| \approx 0.05$ (GeV/c)^2 on the beam proton is seen in the spectrum of fragmentation protons owing to the kinematical correlation]; however, in the SPE region the spectrum should reflect Fermi momentum (and resolution), have a steep slope and no correlation with the beam proton. The one-dimensional correlation function shown as a function of ξ^*_Φ is given in Fig. 3. As can be seen, this function peaks at around 180° and is symmetric, with a dispersion of $\sim$ 50°. Finally, in Figs. 4a and 4b the correlation functions are shown as a function of the summed Cartesian momentum components (x and z) (transverse to the αp relative motion) of the outgoing beam proton and the proton fragment from the α particle. Note the strong signal around 0, the rather symmetric shape and the dispersion of $\sim$ 0.25 (GeV/c) for both spectra.

4. MONTE CARLO SIMULATION

In order to study the shape of the correlation spectra due to the QES process, a simple Monte Carlo simulation was done. We neglected off-shell nuclear effects (binding energy etc.), parametrized the differential elastic pp scattering cross-section as

$$d\sigma/dt \propto e^{bt} \tag{4}$$

with b taken to be 10.3 $(GeV/c)^2$; for the Fermi motion, we assumed a Gaussian distribution with a dispersion of 70 MeV/c [5] in the α rest frame. The resolution of the detector was parametrized as Gaussian with different dispersions in the longitudinal and transverse directions. In Figs. 3 and 4 we also show the result of the simulation. In Fig. 3, the width from the simulation is $\sim 42°$ and, for Figs. 4a and 4b the widths are ~ 0.19 and ~ 0.20 GeV/c, respectively. The smaller widths of the simulated spectra compared with the data are presumably due to neglect of π^0 production processes.

Therefore, to see how much the channel $p + p \rightarrow p + p\pi^0$ widens the spectra, a simple Monte Carlo simulation of this elementary process was performed. The details are given in Appendix B. At $\sqrt{s_{NN}} = 24$ GeV, the inclusive cross-section $\sigma_2(pp \rightarrow \pi^0 X)$ has been measured to be 1.7 ± 1.2 mb [7]. The average number of π^0's detected in that experiment $\langle n_{\pi^0} \rangle$ was 1.0 ± 0.7; therefore we only consider singly produced pions. Let P_D be the probability to produce a π^0 in a pp collision: $P_D = \sigma_2/(\sigma_2 + \sigma_{el}) = 1.7/8.7 = 0.20$ for two-prong events. The probability P_E to have an elastic collision in such events is $P_E = 7/8.7 = 0.80$. The widening of the spectra is calculated from the formula:

$$\sigma = \sqrt{P_D \cdot \sigma_D^2 + P_E \cdot \sigma_E^2}\,, \tag{5}$$

where σ_D is the dispersion due to the π^0 production and σ_E is the dispersion due to the QES process.

From Monte Carlo simulations of the π^0 production process the distribution of azimuthal-angle difference ξ_Φ^* between the two outgoing protons ($|t| > 0.05$) is found to have a dispersion of $\sim 82°$, whereas the distributions of summed transverse-momentum components ξ_x^* and ξ_z^* both have a dispersion of ~ 0.40 GeV/c. Thus inclusion of this process will give a dispersion of $\sim 52°$ for relative azimuthal-angle distributions and ~ 0.25 GeV/c for the summed Cartesian momentum distributions, in fair agreement with the data (see Figs. 3, 4a and 4b).

5. DISCUSSION AND SUMMARY

In an earlier paper [5] we had studied the semi-inclusive momentum distributions of the fragments (p, d, t, ^{3}He) emerging from $\alpha\alpha$ reactions at $\sqrt{s} = 125$ GeV. There it was argued that the p_T distributions of the protons seen with the fragmentation trigger could be explained by QES. Since we have investigated pure break-up reactions, i.e. reactions where no charged pions accompany the fragments, the probability of several nucleon–nucleon (NN) encounters is small (compare the ratio of pp elastic to inelastic cross-section $\sigma_{el}^{pp}/\sigma_{inel}^{pp} \approx 8/32 = 1/4$). From Monte Carlo simulations, the number of QESs per $p\alpha$ collision averaged over the impact parameter is $\langle \nu \rangle_{QES} = 1.05$, i.e. fairly close to unity. This is why we feel rather safe neglecting multiple collisions [8, 9]. The limitation in resolution on the beam-proton side (high rigidity) is the main reason why the correlation functions are so wide. Also the resolution on both sides contributes to smearing of the correlation spectra. It is interesting to note that the trigger conditions used make it possible, in principle, to compare NN scattering in a nuclear medium with that in vacuum (provided the nuclear wave functions are known). The results from our previous publication on this subject [5], taken together with the present work, support a recent fragmentation model based on QES [10]. However, the limited resolution of the detector prevents a comparison of the NN scattering inside and outside nuclear matter.

In conclusion, the QES contribution to the proton fragmentation (pure break-up) channel dominates in the $|t|$ region 0.05–1 $(GeV/c)^2$. The correlation spectra exhibit 'back-to-back'

correlation in the azimuthal plane as well as balancing of the transverse-momentum components of the scattered beam proton and the proton fragment. The 'spectator' proton (Goldhaber process) contributes 16% in this |t| range.

Acknowledgements

The Heidelberg groups were supported by a grant from the Bundesministerium für Forschung und Technologie of the Federal Republic of Germany. The Lund group gratefully acknowledges the support from the Swedish Natural Science Research Council. One of us (M.A.F.) thanks the Deutsche Forschungsgemeinschaft for a Heisenberg fellowship.

REFERENCES

[1] A.S. Goldhaber, Phys. Lett. **53B** (1974) 306.

[2] I.A. Schmidt and R. Blankenbecler, Phys. Rev. **D15** (1977) 3321.

[3] S.E. Koonin, Phys. Rev. Lett. **39** (1977) 680.
R.L. Hatch and S.E. Koonin, Phys. Lett. **81B** (1979) 1.

[4] L. Anderson, W. Brückner, E. Moeller, S. Nagamiya, S. Nissen-Meyer, L. Schroeder, G. Shapiro and H. Steiner, Phys. Rev. **C28** (1983) 1224.

[5] W. Bell et al. (CERN-Heidelberg-Lund Collaboration), Nucl. Phys. **B254** (1985) 475.

[6] W. Bell et al. (CERN-Heidelberg-Lund Collaboration), Phys. Lett. **128B** (1983) 349.

[7] F.T. Dao et al., Phys. Rev. Lett. **30** (1973) 1151.

[8] B. Schürmann, K.M. Hartmann and H.J. Pirner, Nucl. Phys. **A360** (1981) 435.

[9] R.J. Glauber and G. Matthiae, Nucl. Phys. **B21** (1970) 135.

[10] H. Araseki and T. Fujita, Nucl. Phys. **A399** (1982) 434.

[11] P.D.B. Collins, An introduction to Regge theory and high energy physics (The University Press, Cambridge, 1977).

APPENDIX A

LORENTZ TRANSFORMATIONS

Since we are dealing with asymmetric beams, the Lorentz transformations to the c.m.s. can be done either by a general Lorentz transformation and a subsequent rotation or by using simple Lorentz boosts along orthogonal directions. The latter method was preferred. In the laboratory (lab.) frame [5] the beam momenta are given as: $\vec{p}_\alpha = (-p_\alpha \sin\chi,\ p_\alpha \cos\chi,\ 0)$ and $\vec{p}_p = (-p_p \sin\chi,\ -p_p \cos\chi,\ 0)$; where χ is half the beam crossing angle ($\chi = 8.74°$) and $p_\alpha = 62.9$ GeV/c, $p_p = 31.5$ GeV/c are the momenta of the two colliding beams. First, we boost in the x-direction to a frame (′) where the x-momentum component of *each* beam cancels:

$$p'_x = \gamma_x p_x - \eta_x E \tag{1}$$

where $\beta_x \approx -\sin\chi = -0.1519$ and $\gamma_x = 1.0117$ ($\eta_x = \beta_x\gamma_x$). Next, a boost in rapidity (along the y-direction) to the αp c.m.s. (*) is done:

$$y^* = y' - y_{cms} \tag{2}$$

where $y_{cms} = 1/2 \ln [(\Sigma E' + \Sigma p'_y)(\Sigma E' - \Sigma p'_y)] \approx 0.3461$ is the rapidity of the αp c.m.s. as seen from the frame (′). Now the y-momentum components can be obtained in the c.m.s.:

$$p^*_y = m^*_T \sinh(y^*) \tag{3}$$

where m^*_T is the transverse mass: $m^*_T = \sqrt{m^2 + (p^*_x)^2 + (p^*_z)^2} = \sqrt{m^2 + (p'_x)^2 + (p'_z)^2}$.

APPENDIX B

A MODEL FOR SINGLE-π^0 PRODUCTION

We will consider the elementary process $p + p \rightarrow p + X \rightarrow p + p\pi^0$, where X is a diffractively excited object of mass M (X represents a baryon resonance such as Δ^+, N^+, etc.). We will for simplicity assume factorization of the distributions of excited mass $\varrho(M)$ and of four-momentum transfer f(t). Our ansatz is $\varrho(M) \propto M^{-\alpha}$ and $f(t) \propto e^{bt}$ where the values $\alpha = 2$ and $b = 10.3$ $(GeV/c)^2$ were chosen [11]. Once the excited mass M is given, the magnitude of the momentum of that object can be calculated in the pp c.m.s. as $p^*_M = \lambda(s,M^2,m^2)/(2\sqrt{s})$ where $\lambda(x,y,z) = \sqrt{x^2 + y^2 + z^2 - 2xy - 2xz - 2yz}$ and m is the proton mass. From the generated t-value the polar angle can be determined and the azimuthal angle is drawn from a uniform distribution. In this way the momentum vector $\vec{p}^*_M$ is completely determined. The decay $X \rightarrow p + \pi^0$ is assumed to be isotropic in the rest frame of the resonance, and the magnitude of the momentum of the proton (and pion) in that frame is given by $p^R_m = \lambda(M^2,m^2,m_\pi^2)/(2M)$ where m_π is the pion mass. Using Lorentz boosts to the pp c.m.s. the momentum vector $\vec{p}^*_m$ of the proton from the decay can finally be obtained.

Figure captions

Fig. 1 : Double-differential yield $d^2N/d\Phi^*_{pf}d\Phi^*_{pb}$ for detecting the scattered beam proton (pb) at azimuthal angle Φ^*_{pb} and a proton fragment (pf) at azimuthal angle Φ^*_{pf}. The inclined solid line indicates expectation for an ideal QES process (Fermi motion and resolution of the detector ignored) which has 'back-to-back' (anti-)correlation.

Fig. 2a: Yield of proton fragments as a function of p_T^2 for a slice in relative azimuthal angle ξ^*_Φ ($\xi^*_\Phi = \Phi^*_{pb} - \Phi^*_{pf}$; if $\xi^*_\Phi < 0$, then 2π is added). The slice is $\pi/2 < \xi^*_\Phi < 3\pi/2$ which is supposedly the region for QES.

Fig. 2b: Corresponding plot for the regions $\xi^*_\Phi < \pi/2$ and $\xi^*_\Phi > 3\pi/2$. This is the region where 'spectator' (SPE) protons are expected to dominate.

Fig. 3 : The ratio $(dN/d\xi^*_\Phi)_{eve}/(dN/d\xi^*_\Phi)_{mix}$ of proton pairs as a function of relative azimuthal angle ξ^*_Φ. The bin width is 3.6°. Errors are statistical only. The dispersion is ~ 50°. The solid line is the result of a Monte Carlo simulation of the QES process (including Fermi motion and resolution of the detector), giving a dispersion of ~ 42°. The dashed line represents a simulation including π^0 production giving a dispersion of ~ 52°. The experimental data and the latter simulation results are shifted upwards by 4 units for better visibility.

Fig. 4a: The ratio $(dN/d\xi^*_x)_{eve}/(dN/d\xi^*_x)_{mix}$ for proton pairs as a function of summed transverse momentum x-components $\xi^*_x = p^*_{x,pb} + p^*_{x,pf}$. The bin width is 0.04 GeV/c. The dispersion is ~ 0.25 GeV/c. The solid line is the result of a simulation of the QES process giving a dispersion of ~ 0.19 GeV/c. The dashed line is a simulation including π^0 production and its dispersion is about ~ 0.25 GeV/c. The experimental data and the latter simulation results are shifted upwards by 1.6 units.

Fig. 4b: The ratio $(dN/d\xi^*_z)_{eve}/(dN/d\xi^*_z)_{mix}$ of proton pairs as a function of summed transverse momentum z-components $\xi^*_z = p^*_{z,pb} + p^*_{z,pf}$. The bin width is 0.04 GeV/c. The dispersion is ~ 0.25 GeV/c. The solid line is the result of a simulation of the QES process giving a dispersion of ~ 0.20 GeV/c. The dashed line is a simulation including π^0 production and its dispersion is about ~ 0.26 GeV/c. The experimental data and the latter simulation results are shifted upwards by 1.6 units.

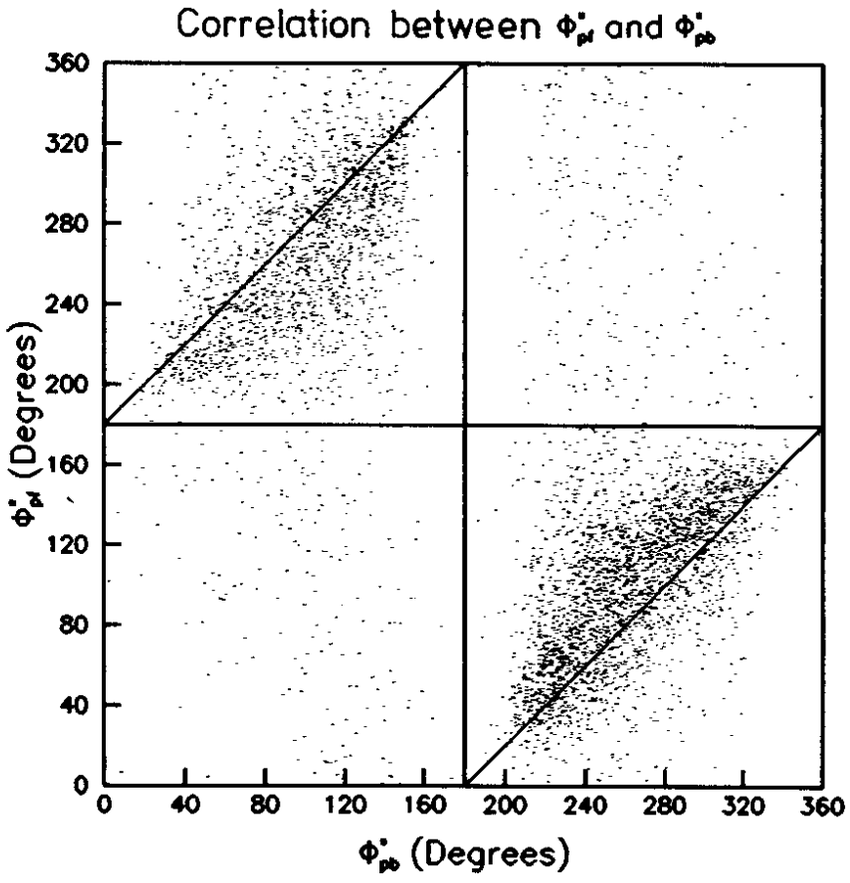
Correlation between Φ^*_{pl} and Φ^*_{pb}
360
320
280
240
200
160
120
80
40
0
Φ^*_{pl} (Degrees)
0
40
80
120
160
200
240
280
320
360
Φ^*_{pb} (Degrees)

Fig. 1

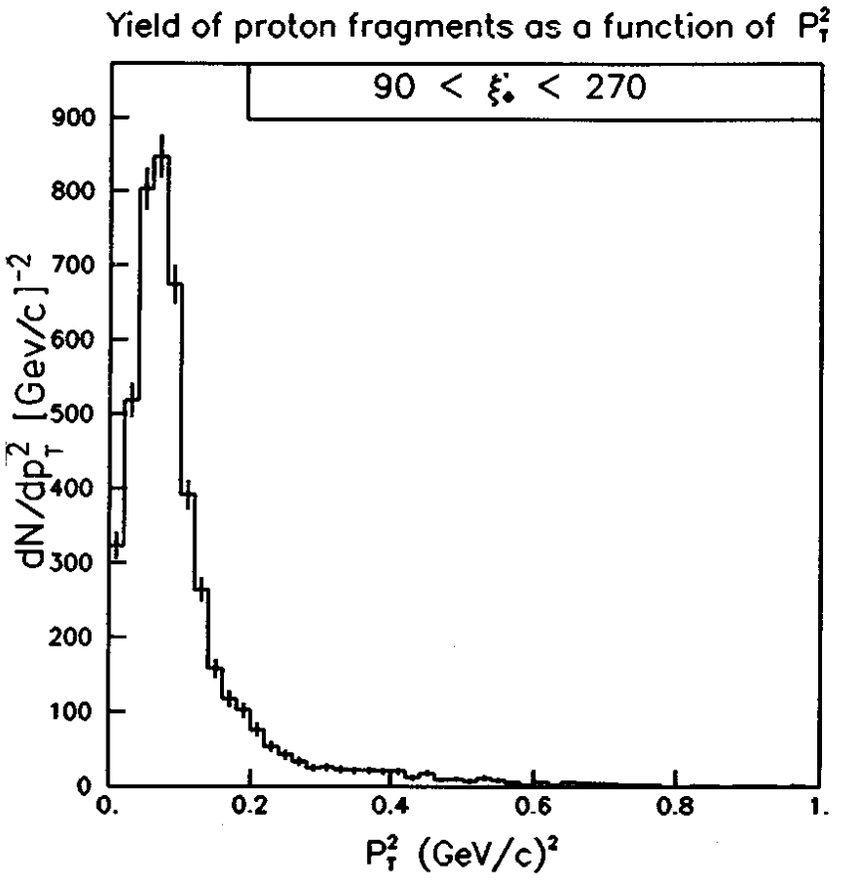
Yield of proton fragments as a function of P_T^2
$90 < \xi_* < 270$
a)
dN/dp_T^2 [Gev/c]$^{-2}$
P_T^2 (GeV/c)^2

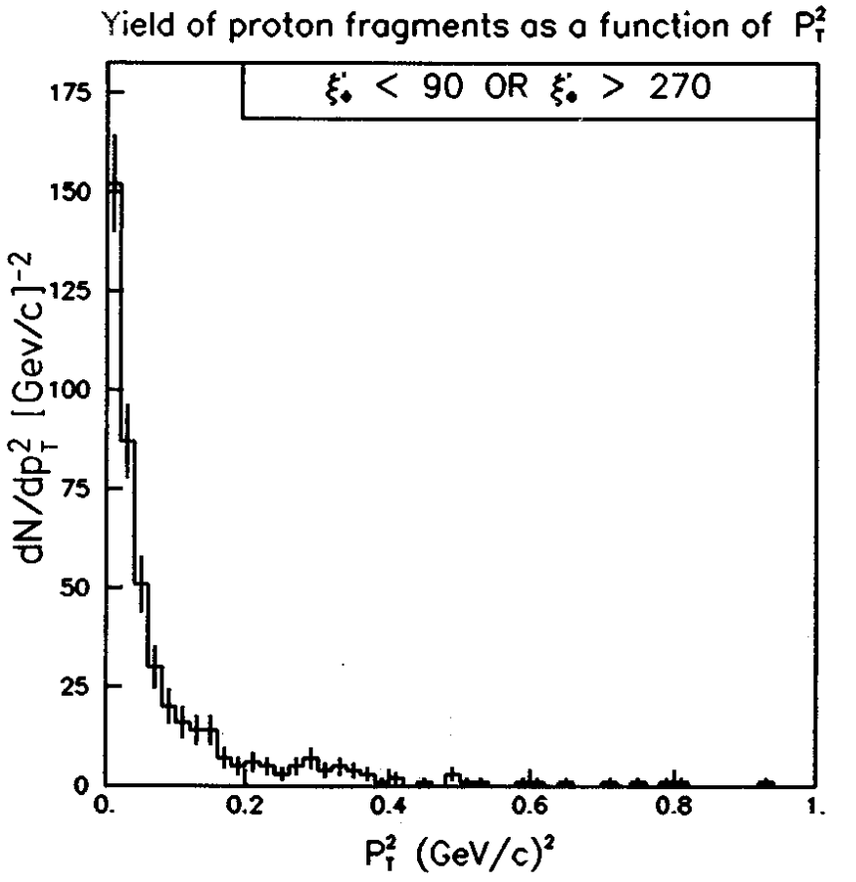
Yield of proton fragments as a function of P_T^2
$\xi_* < 90$ OR $\xi_* > 270$
b)
dN/dp_T^2 [Gev/c]$^{-2}$
P_T^2 (GeV/c)^2

Fig. 2

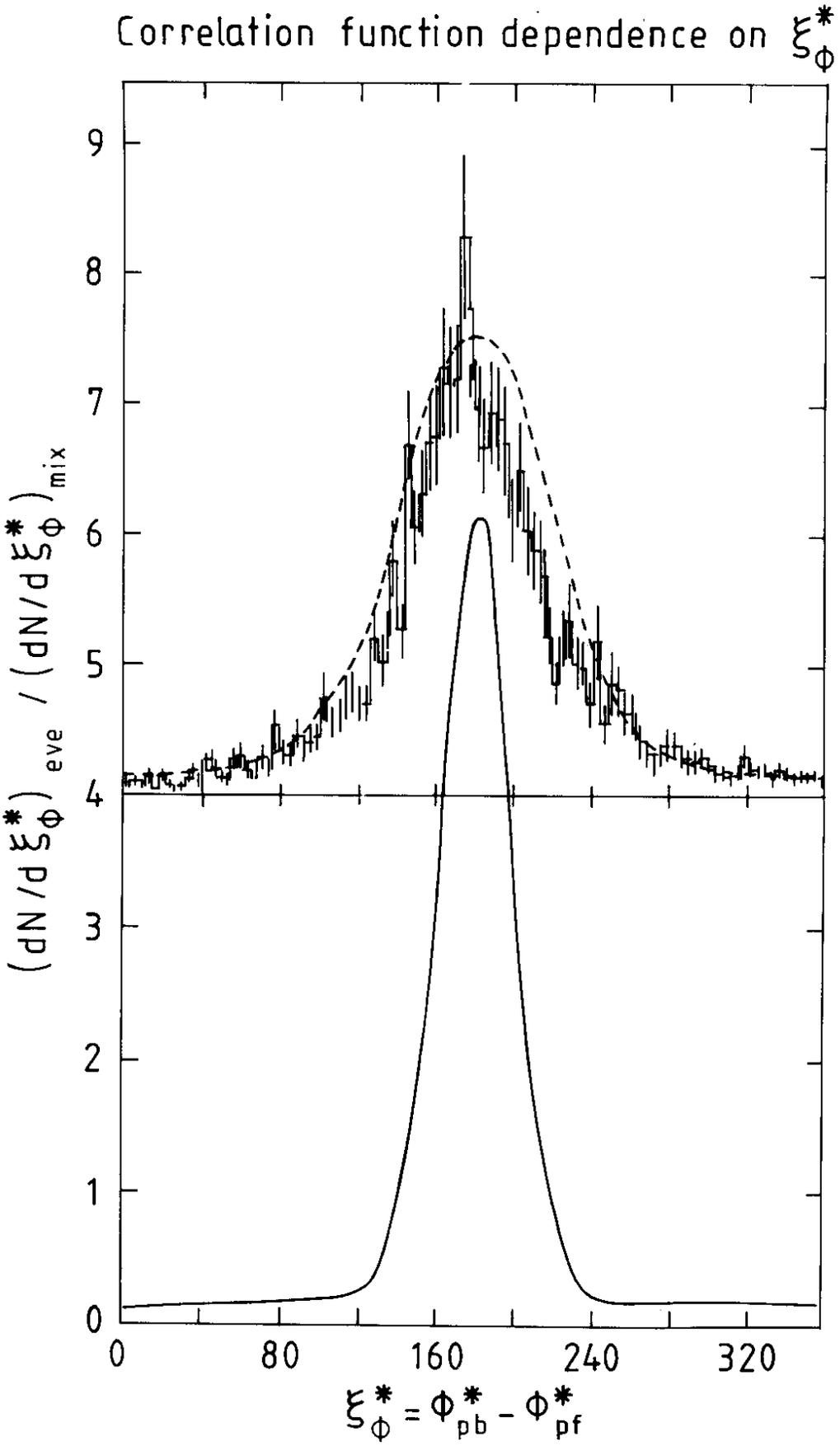
Correlation function dependence on ξ^*_Φ
$(dN/d\xi^*_\Phi)_{eve} / (dN/d\xi^*_\Phi)_{mix}$
$\xi^*_\Phi = \Phi^*_{pb} - \Phi^*_{pf}$
0
1
2
3
4
5
6
7
8
9
0
80
160
240
320

Fig. 3

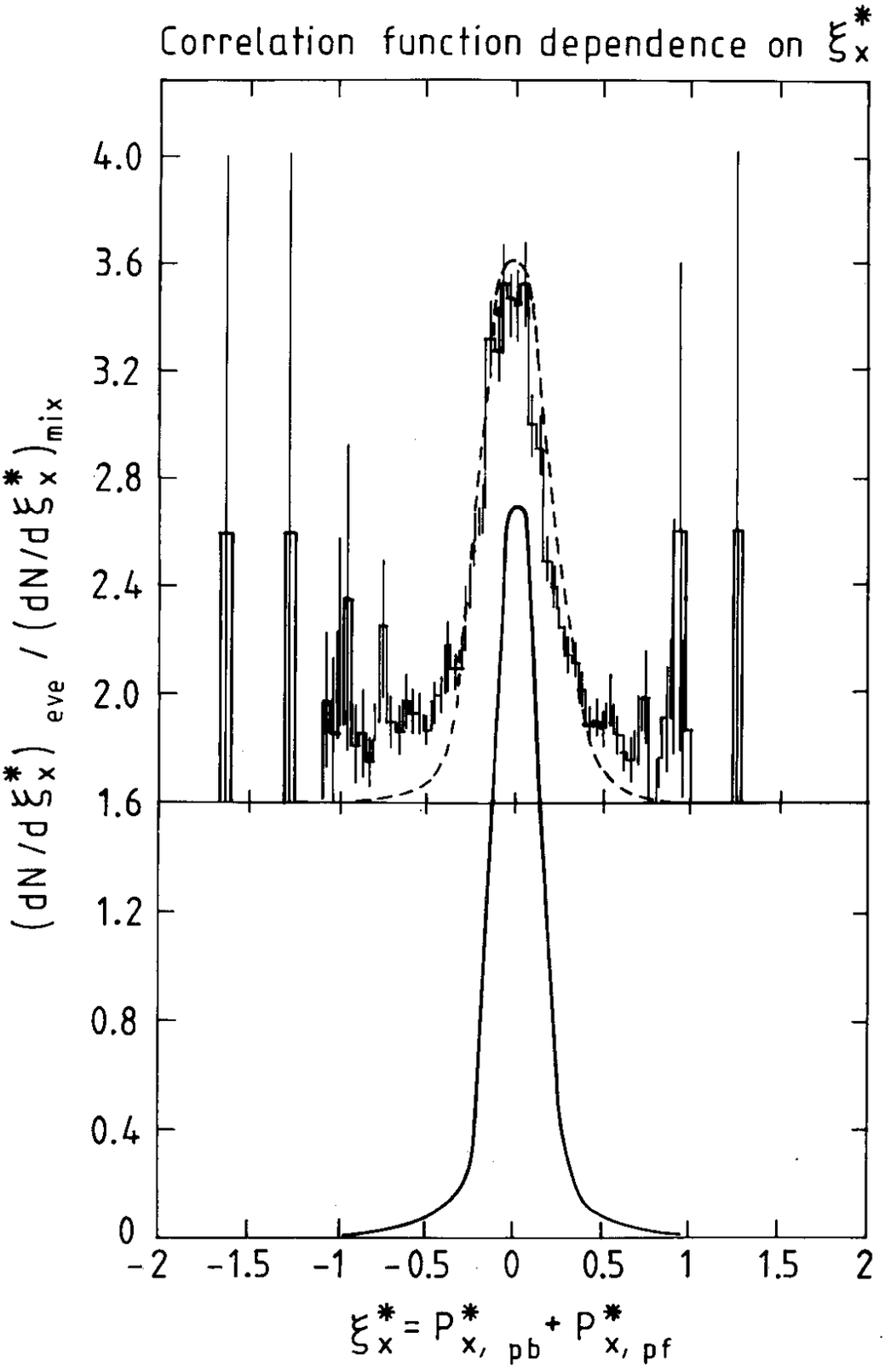
Correlation function dependence on ξ^*_x
$(dN/d\xi^*_x)_{eve} / (dN/d\xi^*_x)_{mix}$
4.0
3.6
3.2
2.8
2.4
2.0
1.6
1.2
0.8
0.4
0
-2
-1.5
-1
-0.5
0
0.5
1
1.5
2
$\xi^*_x = P^*_{x,\,pb} + P^*_{x,\,pf}$

Fig. 4 a)

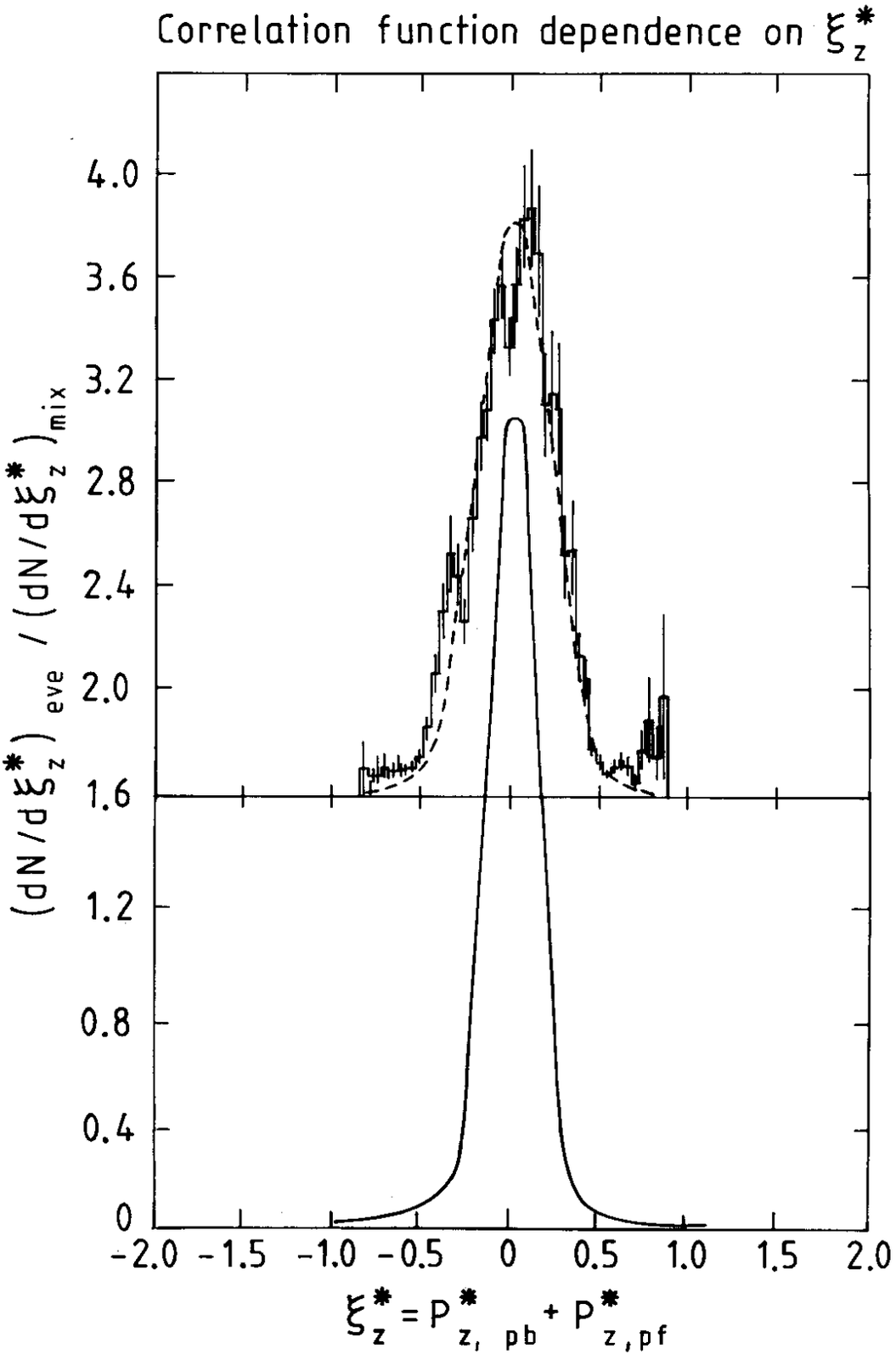
Correlation function dependence on ξ^*_z
$(dN/d\xi^*_z)_{eve} / (dN/d\xi^*_z)_{mix}$
4.0
3.6
3.2
2.8
2.4
2.0
1.6
1.2
0.8
0.4
0
-2.0
-1.5
-1.0
-0.5
0
0.5
1.0
1.5
2.0
$\xi^*_z = P^*_{z,\,pb} + P^*_{z,\,pf}$

Fig. 4 b)